International Journal of Environmental Sciences
ISSN: 2229-7359
Vol. 11 No. 4S, 2025
https://www.theaspd.com/ijes.php

Functionalization Of Photocatalytic Nanomanganese Oxide Particles With *Alpinia Officinarum* For Crystal Violet Degradation

Jeyapaul Ashli [1], Subramanian Priya Velammal [2,*], Thomas Peter amaladhas [3]

[1]*Research Scholar, Reg.No.19232232032009, Department of Chemistry, V. O. Chidambaram College, Tuticorin, Tamil Nadu 628 008, India, Affiliated to Manonmaniam Sundaranar University, Abishekapatti, Tirunelveli-627012, Tamilnadu, India.*

[2]*Associate Professor, Department of Chemistry, V. O. Chidambaram College, Tuticorin, Tamil Nadu 628 008, India, Affiliated to Manonmaniam Sundaranar University, Abishekapatti, Tirunelveli-627012, Tamilnadu, India.*

[3]*Principal, Malankara Catholic College, Mariagiri, Kaliyakkavilai, 629153, Kanyakumari, Tamil Nadu, India.*

[*]*Corresponding author: Priya @ Velammal S, subraja1950@gmail.com.*

Abstract

This investigation presents a facile and environmentally benign approach for the biosynthesis of nanomanganese oxide (Mn_3O_4) particles employing the dried root extract of *Alpinia officinarum*. The electronic spectrum has an absorption maximum centred at 510 nm. FTIR spectral examination confirmed the contribution of phytochemicals such as flavonoids and polyphenolic compounds, which likely functioned as surface-active agents, facilitating both reduction and stabilization of the nanoparticles via interaction with the manganese oxide lattice and formation of O-Mn-O and Mn-O bonds by the presence of vibrational peaks at at 608, 498, and 428 cm^{-1}. XRD analysis revealed characteristic diffraction peaks confirming the formation of a well-defined tetragonal hausmannite manganese oxide lattice structure. SEM imaging demonstrated that the nanoparticles were within the nanoscale range and exhibited irregular morphology with rough surface textures. Elemental analysis via EDX verified the incorporation of manganese (Mn) and oxygen (O) elements. TEM analysis depicted the shape to be elongated rod shaped along with irregular spherical particles and the average size was calculated to be 20.2 nm respectively. The manganese oxide nanoparticles were subjected to catalyse degradation of crystal violet under sunlight and UV-Vis light. The efficiency was evaluated to be 47.98 % and 66.90 % respectively in sunlight and UV-Vis light exposure.

Keywords: Nano manganese oxide particles, *Alpinia Officinarum, Photocatalytic degradation, Crystal violet dye.*

1.INTRODUCTION

Nanotechnology has significantly transformed the field of material science by facilitating the creation of nanomaterials that possess distinctive physical and chemical characteristics. Among these, manganese oxide nanoparticles have gained substantial interest due to their multiple oxidation states, extensive surface area, impressive catalytic performance, and strong redox behaviour. These properties make manganese oxide nanoparticles ideal for a variety of uses, such as in catalysis, energy storage systems, environmental clean-up, and medical applications [1].

Traditional synthesis methods for manganese oxide NPs typically rely on harsh chemicals, elevated temperatures, and energy-demanding procedures, which can be harmful to both the environment and human health. As a more sustainable alternative, green synthesis methods have been developed [2]. These eco-friendly techniques utilize biological materials—namely algae, bacteria, plant extracts and fungi—for reduction and stabilization, adhering to green chemistry principles and providing a safer, more environmentally responsible, and cost-efficient approach.

In particular, plant-based green synthesis leverages naturally occurring compounds—like flavonoids, phenolics, alkaloids, and terpenoids—which serve dual roles in reducing metal ions and stabilizing the resulting nanoparticles. These phytochemicals not only facilitate nanoparticle formation but also enhance surface functionality, leading to improved stability and biological activity [3]. This approach

eliminates the need for toxic chemicals, minimizes waste, and enhances compatibility with biological systems.

Manganese oxide nanoparticles produced via green synthesis have demonstrated considerable effectiveness across several fields. In environmental applications, they serve as adsorbents and photocatalysts capable of removing heavy metals, dyes, and other pollutants. In the energy sector, their high capacity and cycling stability make them valuable for use in supercapacitors and lithium-ion batteries. Additionally, their inherent antimicrobial, antioxidant, and anti-inflammatory properties emphasize their suitability for biomedical purposes, including the development of drug carriers, diagnostic imaging tools, and antibacterial therapies [4][5].

Photocatalytic degradation using manganese oxide nanoparticles represents an advanced oxidative strategy for eliminating organic contaminants from air and water. Due to their broad range of oxidation states, large surface area, and potent redox activity, these nanoparticles efficiently trigger the production of reactive oxygen species, including superoxide ions and hydroxyl radicals —when exposed to light. These ROS actively decompose complex organic pollutants into less toxic substances like CO_2 and H_2O. This green technology is especially effective for breaking down persistent pollutants, including dyes and pharmaceutical residues, positioning manganese oxide NPs as a promising tool for environmental purification and wastewater treatment.

The current study focuses on synthesizing manganese oxide nanoparticles using plant-based approaches and aims to characterize their structural attributes while evaluating their performance in photocatalytic degradation processes.

2. MATERIALS AND METHODS

2.1. Chemicals

Manganese Nitrate Tetrahydrate [$Mn(NO_3)_2 \cdot 4H_2O$] AR, 99% purity and Crystal violet dye AR, 99% purity, obtained from Sisco Research Laboratories, was utilized in its original form without any additional purification. Distilled water was employed for all experimental procedures unless stated otherwise.

2.2. Plant materials

The dried root of brown variety of *Alpinia officinarum* used was sourced from a Siddha medical store in the Thoothukudi district, Tamilnadu, India. Upon identification, the plant was confirmed to be *Alpinia officinarum*. The collected material was thoroughly rinsed several times and then shade dried. After which, it was pulverised and passed through a sieve to ensure uniform particle size. The resulting powdered *Alpinia officinarum* was stored appropriately for subsequent use in extract preparation.

Fig. 1 (a) Manganese (II) nitrate tetrahydrate (b) Dried roots and (c) Fine powder of *Alpinia officinarum*

2.3. Preparation of Manganese oxide nanoparticles using *Alpinia officinarum*

To prepare the plant extract, dried *Alpinia officinarum* root powder and double-distilled water was mixed in 1:10 ratio and maintained at 80 °C for 30 minutes. After heating, the mixture was filtered (Whatman No. 41 filter paper) and the filtrate was labelled and refrigerated at 4 °C for later use.

For the nanoparticle synthesis, the prepared extract and 0.1 M manganese nitrate tetrahydrate [$Mn(NO_3)_2 \cdot 4H_2O$] solution was added in the ratio of 1:1. This mixture was continuously stirred at

80 °C for 1 hour. Precipitate formed during the reaction, was separated via centrifugation, thoroughly rinsed three times with deionized water to eliminate residual impurities, and then heat-treated in a muffle furnace at 600 °C for 2 hours through calcination. This process yielded the final product brown manganese oxide nanoparticles that were gathered and stored for further analysis and application.

Fig 2. *Manganese oxide nanoparticles synthesized using Alpinia officinarum*

2.4. Photocatalytic activity of Manganese oxide nanoparticles

Approximately, 1 ppm crystal violet dye solution in 100 mL was prepared, added with 0.05 g of nanoparticles and placed in stirrer and mixed continuously for 60 min in the dark to establish adsorption and desorption equilibrium of the dye molecules on the nanoparticle surfaces. After this dark phase, the suspension was exposed to direct sunlight, and the dye degradation process was observed over the course of one hour. The degradation rate was determined by analysing the Ultra Violet-Visible spectral analysis of the solution after it was centrifuged and filtered. For the UV light degradation study, a similar procedure was followed and the mixture was then irradiated with UV light in a photoreactor. During the reaction, changes in dye concentration and color were monitored by withdrawing 3 mL samples at 10-minute intervals for up to one hour. These samples were centrifuged and filtered, and the degradation rate was evaluated through UV-Vis spectral analysis.

2.4.1. Degradation efficiency

The photocatalytic degradation efficiency (η) of manganese oxide nanoparticles as a photocatalyst was calculated using the formula:

$$\eta = [(A_0 - A_t) / A_0] \times 100\%$$

where η represents the percentage of dye degradation, the absorbance of dye at time t is given by A_t and the initial absorbance of the dye is represented by A_0.

2.5. Characterization techniques

A range of analytical techniques was employed to characterize the synthesized materials. UV-Visible spectroscopy using a JASCO V-650 spectrophotometer, operated via computer control was used to study optical properties. Structural characterization has been performed using X-ray diffraction (XRD) on an ECO D8 ADVANCE diffractometer, scanning within a 2θ range of 10° to 90°, and crystallite sizes were calculated using the Scherrer formula.

For molecular-level identification, FT-IR data were obtained using a Nicolet iS5 spectrometer. To investigate surface features and particle morphology, SEM was performed with an instrument named Carl Zeiss EVO 18 operating at 15 kV under standard conditions. Through energy-dispersive X-ray spectroscopy (EDAX), using a Quantax 200 system integrated with a Bruker X-Flash detector the

presence of elements was identified.
In addition, high-resolution imaging and internal structural analysis was done using a JEOL JEM-2100 Plus system (TEM).

3.RESULTS AND DISCUSSION

3.1. Ultraviolet-Visible analysis of Nanomanganese oxide particles

Figure 3(a) displays the UV-Visible spectrum of the extract derived from the dried roots. A broad absorption peak is observed near 207 nm and 275 nm, which is likely associated with n–π* and π–π* electronic transitions of the phytochemicals present in the extract. In contrast, Figure 3(b) presents the Ultraviolet-Visible spectrum of manganese oxide nanoparticles synthesized using *Alpinia officinarum*. A distinct absorption band appears around 510 nm, confirming the formation of manganese oxide nanoparticles. This peak is attributed to the electronic excitation from the valence band to the conduction band within the nanoparticles. For instance, in manganese oxide nanoparticles, the bandgap can be affected by the spatial confinement of electrons, leading to an increase in the effective bandgap and influencing the energy required for electronic transitions. Additionally, Mn^{2+}, Mn^{3+}, Mn^{4+} can introduce localized energy levels within the bandgap, further affecting the absorption characteristics and electronic transitions.[6] The initial spectral features near 300 nm are linked to charge transfer transitions from oxide ions (O^{2-}) to manganese ions in the +2 and +3 oxidation states (Mn^{2+} and Mn^{3+}). The subsequent bands are more plausibly associated with *d–d* crystal field transitions involving octahedrally coordinated Mn^{3+} ions. These transitions include $^3E_g(G) \leftarrow {}^3T_{1g}$, $^3A_{2g}(F) \leftarrow {}^3T_{1g}$, $^3A_{2g}(G) \leftarrow {}^3T_{1g}$, $^3T_{2g}(H) \leftarrow {}^3T_{1g}$, $^3T_{1g}(H) \leftarrow {}^3T_{1g}$, and $^3E_g(H) \leftarrow {}^3T_{1g}$. This spectral pattern bears a close resemblance to that observed by Boyero et al. for the hausmannite phase [7]. As the particle size decreases, quantum confinement effects become more pronounced, leading to shifts in absorption peaks and changes in electronic transition energies. These UV-Visible spectral features collectively validate the successful fabrication of nanomanganese oxide particles.

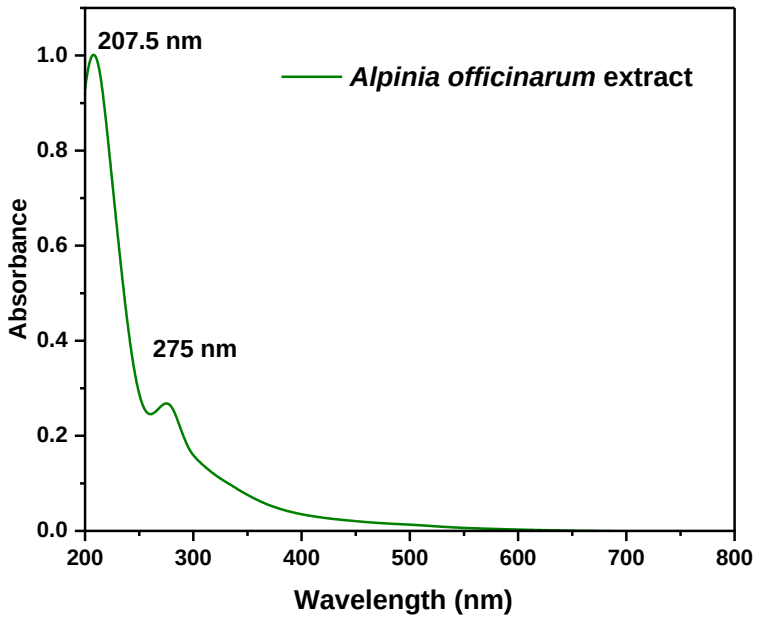

Fig.3 (a) *The Ultraviolet-Visible spectrum of Alpinia officinarum dried root extract*

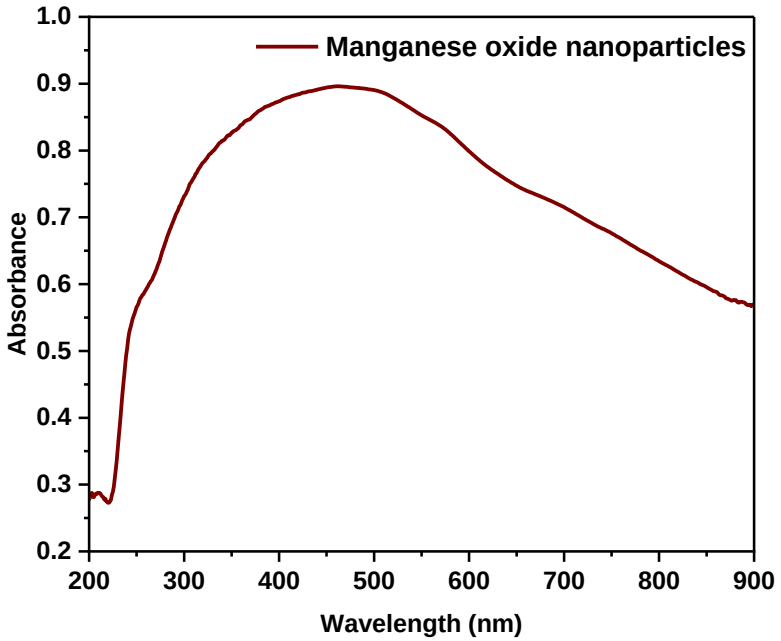

Fig.3 (b) *Ultraviolet-Visible Absorption spectra of Alpinia officinarum functionalized Manganese oxide nanoparticles*

3.2. FTIR studies of Nanomanganese oxide particles

Figure 4(a) displays the FTIR spectrum of dried *Alpinia officinarum* root extract. A broad peak around 3000 cm^{-1} corresponds to –OH and –NH stretching from amino acids. The sharp peak centred at 1637 cm^{-1} is linked with C–O and N–O stretching from ester groups, while the 1400 cm^{-1} peak arises from C–C stretching in aromatic alkaloids. Three peaks in fingerprint region (~1100 cm^{-1}) reveals vibrations related to –CH deformation and C–O/C–C vibrational modes, signalling the existence of polyphenols and flavonoids. Figure 4(b) exhibits the FTIR spectrum of nanomanganese oxide particles synthesized using the plant extract. A broad peak near 3450 cm^{-1} signifies hydroxyl group vibrations from acids. The 1629 cm^{-1} peak indicates shift in the peak corresponding to C-O and N-O vibrations in the plant extract. While the peak at 1400 cm^{-1} might be from the C-C vibrations of aromatic alkaloids and the weak peak between 1500–1000 cm^{-1} could be assigned to phytoconstituents that corroborates its capping nature. Peaks at 608, 498, and 428 cm^{-1} correspond to O–Mn–O and Mn–O stretching, with their broadness indicating nano crystallinity. The findings verify that manganese oxide nanoparticles have been synthesized, with plant-derived phytochemicals serving as inherent stabilizing agents.

International Journal of Environmental Sciences
ISSN: 2229-7359
Vol. 11 No. 4S, 2025
https://www.theaspd.com/ijes.php

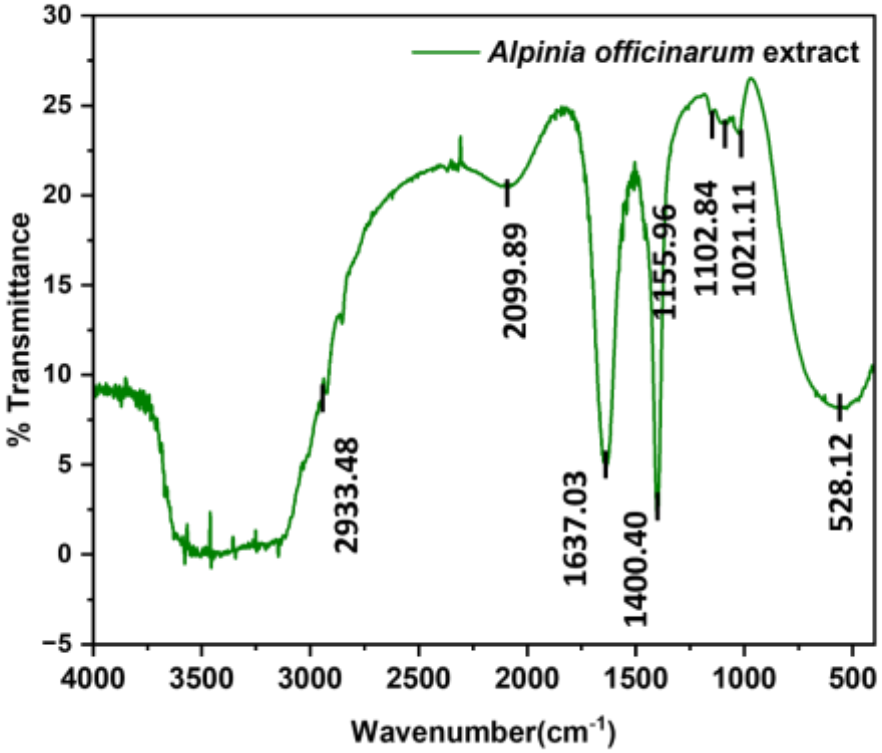

Fig.4 (a) *FTIR spectrum of Alpinia officinarum extract*

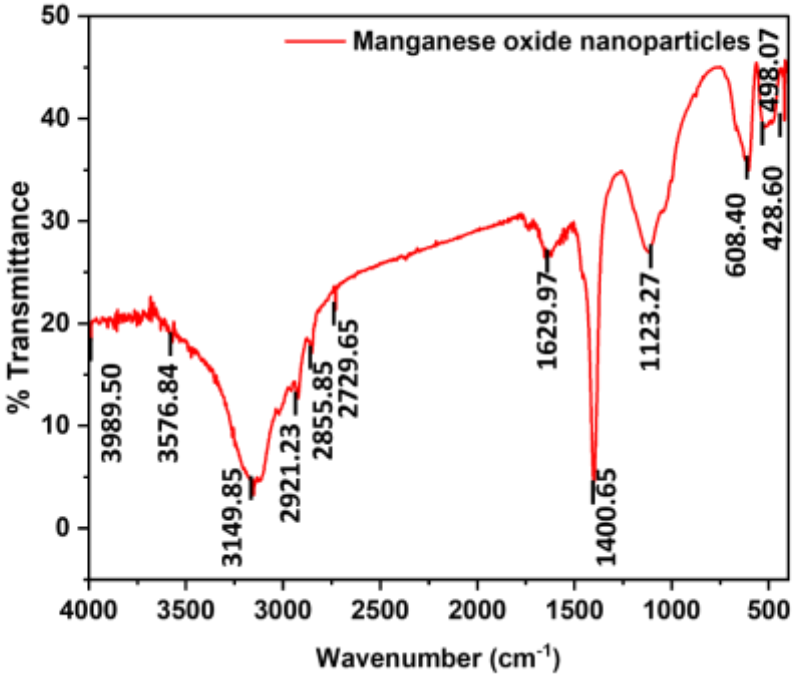

Fig.4 (b) *FTIR spectrum of Alpinia officinarum functionalized Nanomanganese oxide particles.*

3.3.XRD

Figure 5 presents the XRD pattern of the calcined manganese oxide, displaying distinct diffraction peaks typical of nanocrystalline manganese oxide. Peaks are present at 2θ values of 17.9^0, 28.8^0, 32.2^0, 35.9^0, 37.8^0, 44.3^0,50.6^0, 58.4^0, 59.7^0, 64.5^0 that corresponds to 101, 112, 103, 211, 004, 220, 105, 321, 224, 400 planes respectively. These peaks correspond to the hausmannite Mn_3O_4 - tetragonal phase, consistent to the JCPDS card number 24-0734. The XRD results clearly confirm the successful synthesis of nanomanganese oxide particles. [8-11]

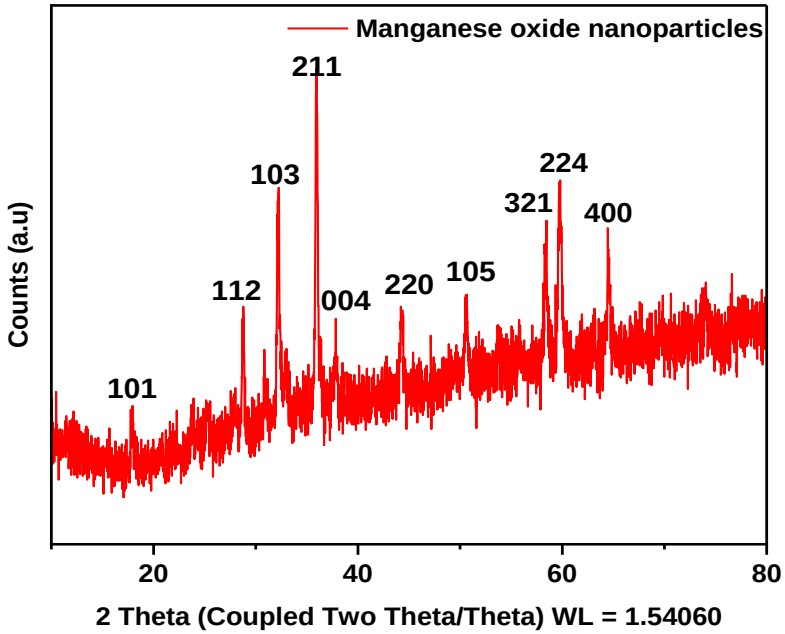

Fig.5 XRD *pattern of Alpinia officinarum functionalized Nanomanganese oxide particles*

3.4. SEM and EDAX Analysis

Figures 6(a–d) present SEM images of these manganese oxide nanoparticles. The micrographs reveal that the nanoparticles are highly crystalline with rough surfaces and exhibit particle agglomeration. This clustering likely results from the nanoparticles' large specific surface area and elevated surface energy. Additionally, the aggregation may be influenced by the drying process during synthesis. Figure 7 displays the EDAX spectrum of the manganese oxide nanoparticles produced with *Alpinia officinarum* extract. The EDAX results indicate an elemental composition of 65.24 atomic percent oxygen and 34.76 atomic percent manganese. This confirms the presence of both manganese and oxygen within the synthesized nanoparticles. The detailed elemental composition is summarized in Table 1.

International Journal of Environmental Sciences
ISSN: 2229-7359
Vol. 11 No. 4S, 2025
https://www.theaspd.com/ijes.php

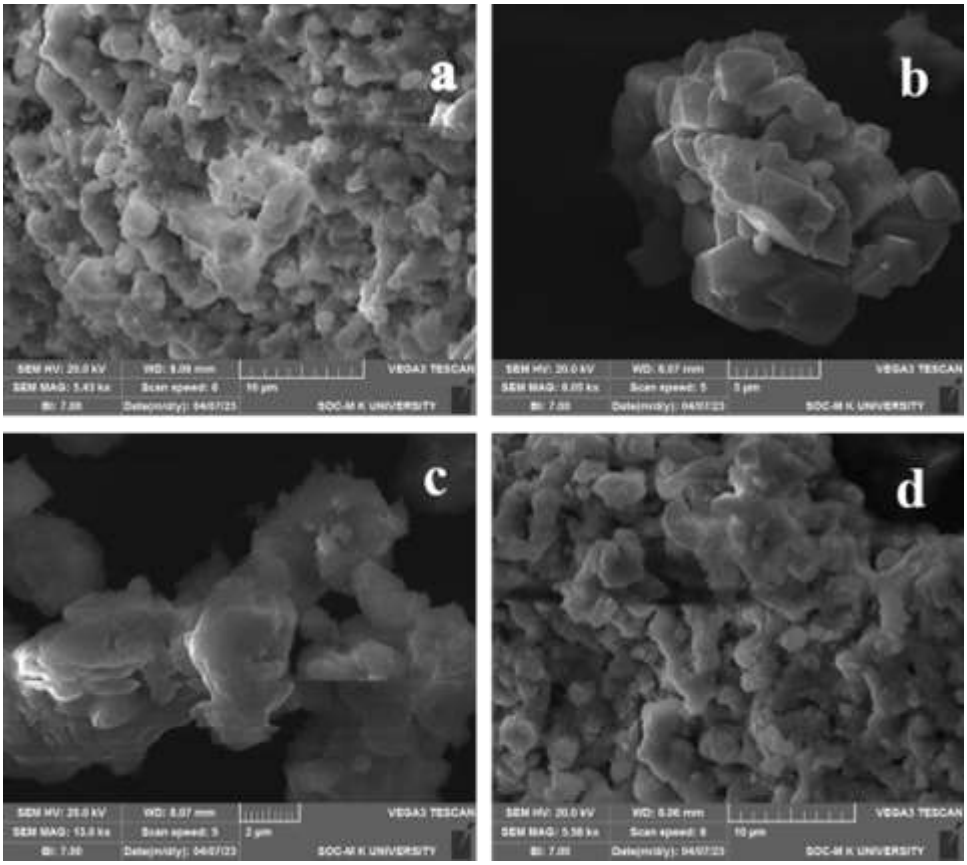

Fig.6 (a-d) *SEM images of Manganese oxide nanoparticles at different magnifications*

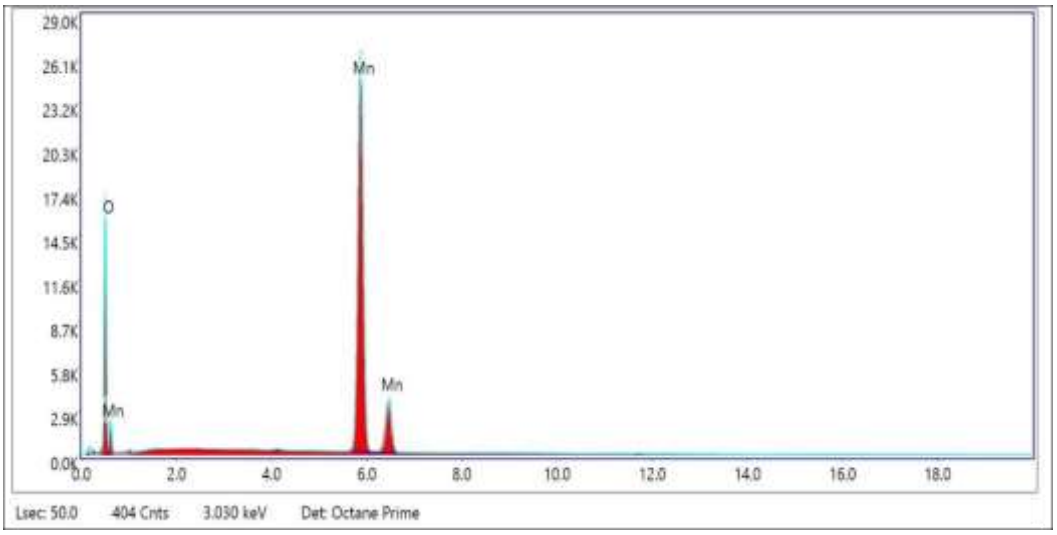

Fig.7 Elemental *composition of Manganese oxide nanoparticles*

Table 1 *Elemental composition of Alpinia officinarum functionalized Nanomanganese oxide particles*

Element	Weight %	Atomic %	Net Int.	Error %	Kratio	Z	A	F
O K	37.07	65.24	1678.80	6.52	0.1736	1.1395	0.4471	1.0000
MnK	62.93	34.76	7174.11	1.05	0.5465	0.9012	1.0077	1.0040

International Journal of Environmental Sciences
ISSN: 2229-7359
Vol. 11 No. 4S, 2025
https://www.theaspd.com/ijes.php

3.5. TEM studies

As depicted in Figure 8 (a-d), the nanoparticles exhibit a combination of distorted spherical and elongated rod like morphology. The TEM analysis demonstrated that the nanomanganese oxide particles have a mean size of approximately 20.2 nm as shown in fig.8 (e). This variation in shape suggests the influence of phytochemicals from the *Alpinia officinarum* extract during the synthesis process, which may act as directing and stabilizing agents.

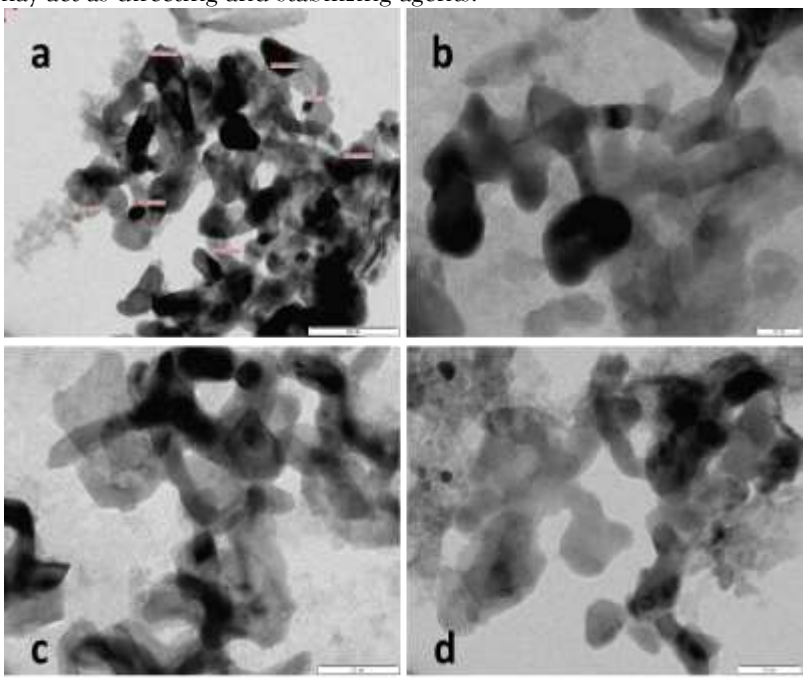

Fig.8 (a-d) *TEM images of Manganese oxide nanoparticles*

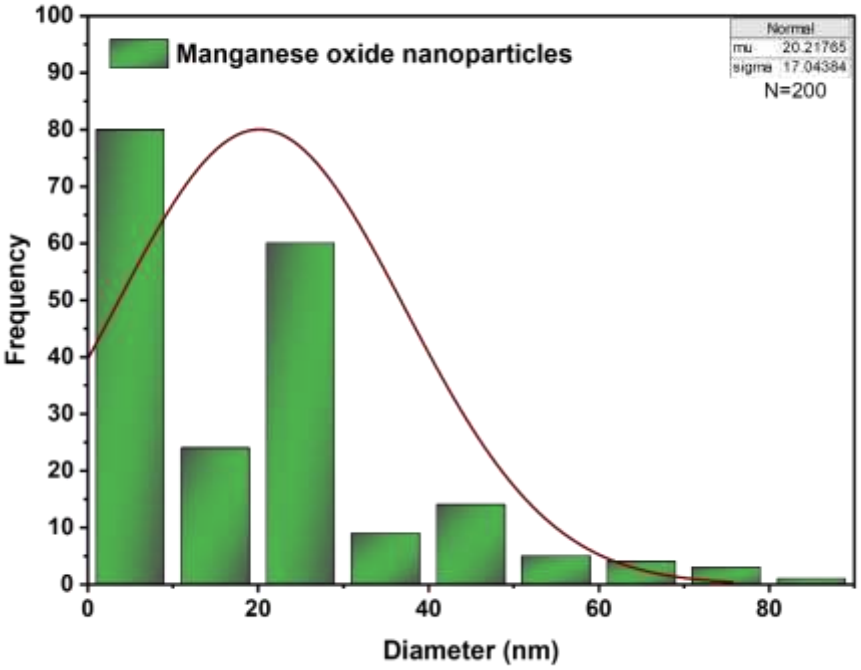

Fig.8 (e) *Particle size distribution*

3.6. Crystal violet photocatalytic degradation

The photocatalytic efficiency of manganese oxide nanoparticles synthesized with *Alpinia officinarum* root extract was assessed by monitoring the decolouration of crystal violet dye using a UV-Visible spectrophotometer [12]. Upon Ultraviolet-Visible irradiation, photons striking the surface of the manganese oxide nanoparticles excite electrons (e^-) electrons are excited from the valence band to the conduction band, resulting in the formation of positively charged holes (h^+) within the valence band. These holes subsequently react with water molecules adsorbed on the surface (H_2O) to generate reactive species like hydroxyl (OH) radicals, which then react with the dye molecules, leading to their breakdown [13].

The Ultraviolet-Visible absorbance spectrum corresponding to the solution of pure crystal violet (Fig. 9) exhibits a prominent absorption peak at 583 nm, corresponding to the dye's chromophore, and an additional peak at 300 nm attributed to aromatic benzene rings. The absorbance at 583 nm served as the key indicator for monitoring the photocatalytic degradation.

Photo degradation experiments were conducted by mixing the dye solution with manganese oxide nanoparticles and exposing the mixture to sunlight and UV light separately for one hour. Over the 60-minute irradiation period, the absorption peak intensity gradually diminished. The reduction in the 583 nm peak intensity indicates the breakdown of the dye's chromophore responsible for its violet colour. Furthermore, the cleavage of benzene and heterocyclic rings causes disruption of aromatic bonds, accelerating the decolourization process. After one hour of irradiation, crystal violet dye degraded to some extent was observed under both sunlight and UV-Vis light, as depicted in Figures 10 and 11. Figures 10 and 11 illustrate the changes in absorbance spectra and the photocatalytic quenching efficiency of manganese oxide nanoparticles synthesized from *Alpinia officinarum* extract under sunlight and UV-Vis irradiation, respectively. The dye's colour visibly faded after 60 minutes of exposure in both conditions, as summarized in Tables 2 and 3.

3.6.1. Degradation efficiency:

The degradation efficiency was determined as a percentage using the following equation:

$$\text{Percentage Efficiency} = [(A_0 - A_t) / A_0] \times 100\%$$

where A_0 represents the initial absorbance of the dye and A_t is the absorbance at various time intervals. Analysis of the absorbance spectra revealed that manganese oxide nanoparticles achieved a maximum degradation efficiency of 47.98% under 60 minutes of sunlight exposure and 66.90% under UV light irradiation. These findings indicate that the light-driven catalytic activity of nanomanganese oxide particles is significantly enhanced under UV-Vis light compared to direct sunlight and experiments could be repeated by varying pH, concentration of nanoparticle and crystal violet dye. The absorbance data and corresponding degradation efficiencies for both sunlight and UV exposure are presented in Tables 2 and 3, respectively. Figure 12 illustrates a contrasting photocatalytic degradation efficiencies of manganese oxide nanoparticles in UV-Vis and sunlight, clearly demonstrating superior dye degradation under UV-Vis irradiation.

International Journal of Environmental Sciences
ISSN: 2229-7359
Vol. 11 No. 4S, 2025
https://www.theaspd.com/ijes.php

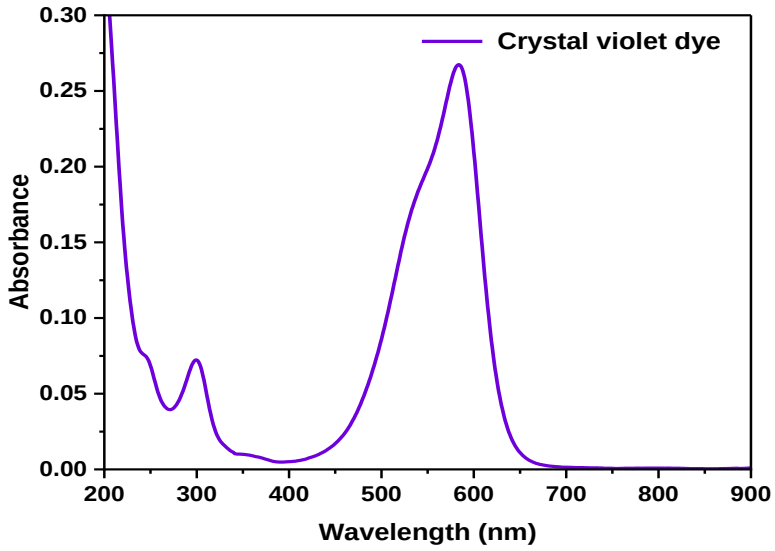

Fig.9. *Ultraviolet-Visible absorption spectra of pure crystal violet dye*

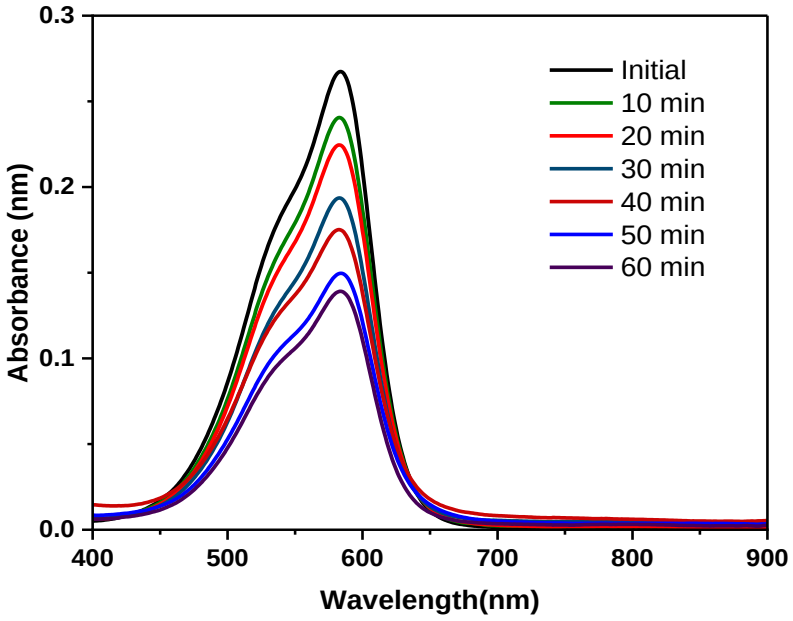

Fig.10. *Ultraviolet-Visible absorption spectra of sunlight treated crystal violet dye*

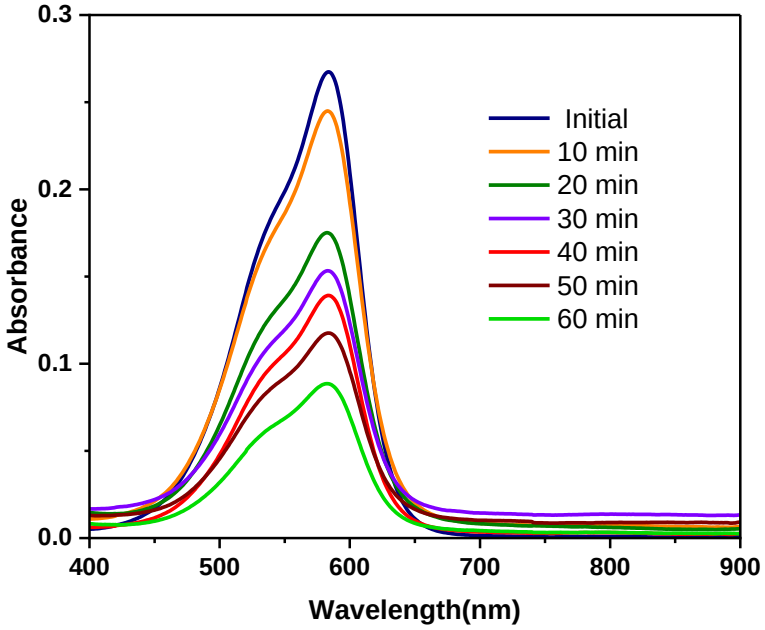

Fig.11. *Ultraviolet-Visible absorption spectra of crystal violet dye under ultraviolet visible irradiation*

Table.2. *Absorbance values and degradation efficiency of Manganese oxide nanoparticles synthesized using Alpinia officinarum root extract under sunlight*

Time (min)	Degradation by Manganese oxide nanoparticles under direct sunlight	
	Absorbance	Efficiency (%)
Initial	0.2674	-
10 min	0.2405	10.05
20 min	0.2246	16.00
30 min	0.1936	27.50
40 min	0.1751	34.52
50 min	0.1497	44.02
60 min	0.1391	47.98

Table.3. *Absorbance values and degradation efficiency of Manganese oxide nanoparticles synthesized using Alpinia officinarum root extract under UV-Vis radiation*

Time (min)	Degradation by Manganese oxide nanoparticles under UV-Vis radiation	
	Absorbance	Efficiency (%)
Initial	0.2674	-
10 min	0.2450	8.38
20 min	0.1745	34.74
30 min	0.1533	42.67
40 min	0.1385	48.20
50 min	0.1176	56.02
60 min	0.0885	66.90

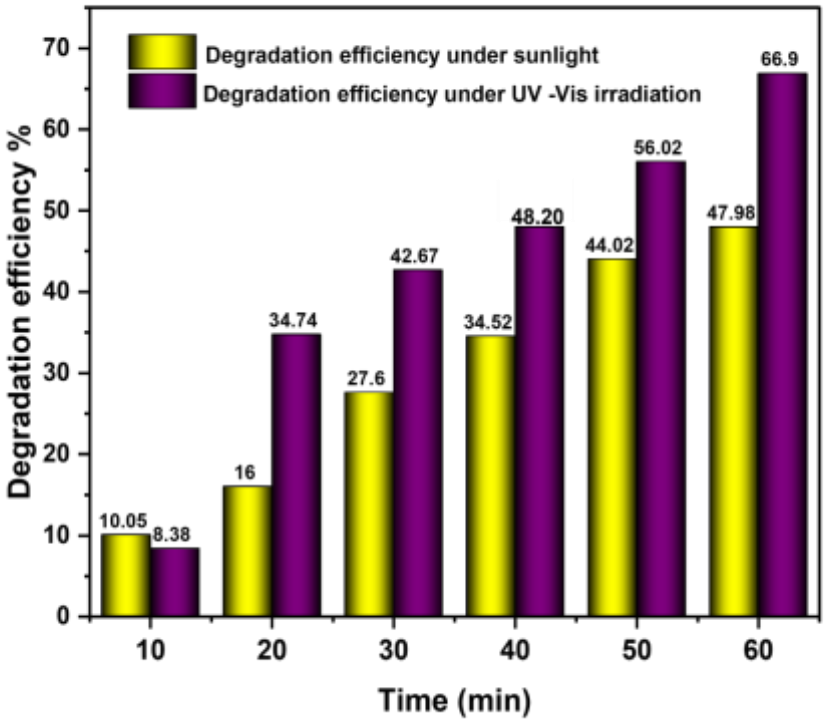

Fig.12.*Comparison of Degradation efficiency of Manganese oxide nanoparticles under sunlight and UV irradiation*

4.CONCLUSION

This research highlights the successful development of manganese oxide (Mn_3O_4) nanoparticles using an environmentally benign green synthesis method. By employing plant-based or natural reducing agents, the synthesis process aligns with principles of green chemistry. Resulting nanoparticles displayed favourable structural and morphological characteristics that was confirmed by various characterisation techniques, making them suitable for photocatalytic applications. Nano Mn_3O_4 particles was employed in photocatalytic degradation to demonstrate the degradation of organic pollutants under UV light. Their notable performance in breaking down contaminants confirms their potential as effective catalysts in water purification processes. In addition to their strong photocatalytic activity, the nanoparticles showed promising reusability and stability, reinforcing their value for sustainable environmental applications. Overall, this study establishes green-synthesized manganese oxide nanoparticles as viable materials for eco-friendly photocatalytic degradation. Their low environmental impact, coupled with high efficiency, positions them as attractive alternatives for addressing pollution in aqueous environments. Future research should aim to explore their behaviour in real-world conditions, optimize synthesis parameters, and further investigate the degradation mechanisms involved.

5.REFERENCE

1. Lu, X., & Zhao, C. (2015). Nanostructured Mn-based oxides for electrochemical energy storage and conversion. *Nano Energy*, 10, 315–334.

2. Iravani, S. (2011). Green synthesis of metal nanoparticles using plants. *Green Chemistry*, 13(10), 2638–2650.

3. Singh, J., Dutta, T., Kim, K.-H., Rawat, M., Samddar, P., & Kumar, P. (2018). 'Green' synthesis of metals and their oxide nanoparticles: Applications for environmental remediation. *Journal of Nanobiotechnology*, 16(1), 84.

4. Dutta, P., Pal, S., & Seehra, M. S. (2012). Size and structure of Mn_3O_4 nanoparticles from X-ray scattering and magnetic measurements. *Journal of Applied Physics*, 112(6), 064310.

5. Ameen, S., Akhtar, M. S., Song, M., & Shin, H. S. (2014). Green synthesis of manganese oxide nanostructures and their application in battery and biomedical systems. *Materials Letters*, 120, 267–270.

6. Ghosh SK. Diversity in the Family of Manganese Oxides at the Nanoscale: From Fundamentals to Applications. ACS Omega. 2020 Oct 5;5(40):25493-25504. doi: 10.1021/acsomega.0c03455. PMID: 33073076; PMCID: PMC7557223.

7. J.M. Boyero, E.L. Fernández, J.M. Gallardo-Amores, R.C. Ruano, V.E. Sánchez, E.B. Pérez, Int. J. Inorg. Mater. 3 (2001) 889.

8. Raj, AME, Victoria, SG, Jothy, VB, Ravidhas, C, Wollschlager, J, Suendorf, M, Neumann, M, Jayachandran, M & Sanjeeviraja, C, 2010, 'XRD and XPS characterization of mixed valence Mn_3O_4 hausmannite thin films prepared by chemical spray pyrolysis technique', Applied Surface Science, vol. 256, no. 9, pp. 2920-2926.

9. Raj, BGS, Asiri, AM, Wu, JJ & Anandan, S, 2015, 'Synthesis of Mn_3O_4 nanoparticles via chemical precipitation approach for supercapacitor application', Journal of Alloys and Compounds, vol. 636, pp. 234-240.

10. Dhaouadi, H, Madani, A & Touati, F, 2010, 'Synthesis and spectroscopic investigations of Mn_3O_4 nanoparticles', Materials Letters, vol. 64, no. 21, pp. 2395-2398.

11. Wang, L, Li, Y, Han, Z, Chen, L, Qian, B, Jiang, X, Pinto, J & Yang, G, 2013, 'Composite structure and properties of Mn_3O_4/graphene oxide and Mn_3O_4/graphene', Journal of Materials Chemistry A, vol. 1, pp. 8385-8397.

12. Taghavi Fardood, S., Moradnia, F., Yekke Zare, F. *et al.* Green synthesis and characterization of α-Mn_2O_3 nanoparticles for antibacterial activity and efficient visible-light photocatalysis. *Sci Rep* **14**, 6755 (2024). https://doi.org/10.1038/s41598-024-56666-2.

13. Manita Khatri, Aakash Gupta, Kabita Gyawali, Anup Adhikari, Agni Raj Koirala, Niranjan Parajuli, Photocatalytic degradation of dyes using synthesized δ-MnO2 nanostructures, Chemical Data Collections, Volume 39, 2022, 100854, ISSN 2405-8300, https://doi.org/10.1016/j.cdc.2022.100854.